Effects of small recoil momenta in one-photon two-electron ionization

M. Ya. Amusia,[1,2] E. G. Drukarev,[1,3] E. Z. Liverts,[1] and A. I. Mikhailov[3]
[1]*The Racah Institute of Physics, The Hebrew University of Jerusalem, Jerusalem 91904, Israel*
[2]*A. F. Ioffe Physical-Technical Institute, St. Petersburg 194021, Russia*
[3]*B. P. Konstantinov Petersburg Nuclear Physics Institute, Gatchina, St. Petersburg 188300, Russia*
(Received 16 January 2013; published 22 April 2013)

We calculate the distributions in recoil momenta and the energy distributions for the high-energy nonrelativistic double photoionization of helium caused by the quasifree mechanism of the process. The distributions obtain local maxima at small values of the recoil momenta. This is in agreement with the earlier predictions and with recently obtained experimental data. We obtained also the angular correlations, which reach the largest value in the "back-to-back" configuration of the photoelectrons. Our analysis is valid in all high-energy nonrelativistic region. Particular equations are true up to the photon energies making several kilo-electron-volts. We present numerical results for the photon energies in the region of 1 keV, employed in the recent experiments.

DOI: 10.1103/PhysRevA.87.043423 PACS number(s): 32.80.Fb, 34.80.Dp, 31.15.V−

I. INTRODUCTION

The recent measurement of the yield of double-charged ions in photoionization of helium [1–3] confirmed the existence of the quasifree mechanism (QFM) of the double photoionization which was predicted in [4]. The differential cross sections of the double photoionization were calculated earlier in a number of papers [4–9], where the authors studied the distributions in characteristics of each photoelectron. In the pioneering experiments [1–3], the distribution in momentum transferred to the nucleus q (recoil momentum) was measured. Thus the problem of calculation of such distributions as $d\sigma^{2+}/dq^2d\varepsilon$ with ε the energy of one of the photoelectrons and $d\sigma^{2+}/dq^2$ became actual.

In the present paper we calculate these differential cross sections for the double photoionization of helium at high values of the photon energies, corresponding, however, to nonrelativistic energies of the photoelectrons. We present the results for the differential cross sections $d\sigma^{2+}/dq^2d\varepsilon$. We trace the dependence of these characteristics on the photon energy ω.

Recall that the experiments [1–3] in which the photons carried the energies 450, 800, and 900 eV demonstrated that the distribution of outgoing electrons obtains a surplus at small q of about 2 a.u.. The kinematics of these experiments enables the separation of the nondipole contributions at small values of q. Thus the observed surplus is entirely due to the nondipole terms.

By that time, only two mechanisms of the process were known. In both of them the electron which interacted with the photon directly obtained almost all the incoming photon energy ω. In the first one, known as the shakeoff, the secondary electron is pushed to continuum by the sudden change of the effective field. In the second, called the *knockout* mechanism, the photoelectron inelastically collides with the bound one, sharing the photon energy. Both mechanisms contain the single photoionization as the first step. This process cannot take place on a free electron. Thus the momentum q, which is transferred in this step to the nucleus, strongly exceeds the averaged momentum of the bound electron μ, in the case of the high-energy photon

$$\omega \gg I \tag{1}$$

(I is the single-particle ionization potential). Of course, there is a configuration in which the second electron transfers momentum $q_1 \gg \mu$ such that $|\mathbf{q}+\mathbf{q_1}| \sim \mu$. However, since each act of transferring a large momentum $q \gg \mu$ leads to an additional small factor [10,11], its probability is very small. The distribution $d\sigma^{2+}/dq^2d\varepsilon$ provided by these two mechanisms peaks at $q \approx (2m\omega)^{1/2} \gg \mu$ (m is the electron mass), becoming very small at $q \sim \mu$. This remains true beyond the dipole approximation.

In contrast to a single-electron case, the two electrons can absorb a photon without participation of the nucleus. In the free process, $\mathbf{q}=0$. In the QFM small momentum $q \sim \mu$ is transferred to the nucleus, i.e., q is much smaller than the momenta of the outgoing electrons. The distributions $d\sigma^{2+}/dq^2d\varepsilon$ and $d\sigma^{2+}/dq^2$ the have local maxima at small q of the order of μ. That is what was detected in [1–3].

Momentum $\mathbf{q}$ transferred to the nucleus can be written as

$$\mathbf{q} = \mathbf{k} - \mathbf{p_1} - \mathbf{p_2}, \tag{2}$$

where $\mathbf{p}_{1,2}$ are momenta of the outgoing electrons, while $\mathbf{k}$ is that of the photon. The recoil momentum q can become small only if the large momenta of the outgoing photoelectron with $p_i = |\mathbf{p}_i| \ll \mu$ compensate each other to a large extent ($k = |\mathbf{k}|$ is always much smaller than p_i while we consider the photon energies, corresponding to nonrelativistic photoelectrons). Hence the values of p_i should be close, i.e., $p_1 \approx p_2 \approx \sqrt{mE}$ with E the sum of the energies of the photoelectrons. Thus in QFM the bound electrons exchange by small momentum $q \sim \mu$ with the nucleus and by large momentum of the order $p_i \gg \mu$ between themselves.

We calculate the amplitude of the QFM in the lowest order of expansion in powers of q/p_i. This corresponds to expansion of the bound state wave function in the lowest order in powers of r_{12}/r_i, with r_i standing for the distance between the electron and the nucleus, while r_{12} is the interelectron distance. We consider the high-energy photons, corresponding, however, to nonrelativistic energies of the outgoing electrons. Thus we assume that $\omega \ll m$. Keeping in mind future extension of the analysis to the relativistic case, we employ the relativistic units $\hbar = c = 1$.

Since $q \sim \mu$ the higher terms of expansion in powers of q/p_i are of the same order as those coming from the interactions between the photoelectrons and the nucleus. However, they are of quite different physical origin. Thus we include interactions of the nucleus with the electrons exactly, describing the latter by the nonrelativistic functions of the Coulomb field. Interaction between the outgoing electrons is proportional to the square of its Sommerfeld parameter $\xi_{ee} = \alpha/v$, where v is their relative velocity. For the energies of the order 1 keV employed in the experiments [1–3], this interaction provides a correction of the order of 2% and can be neglected.

Direct relation of the QFM to the behavior of the bound state wave function $\Psi(r_1,r_2,r_{12})$ at small distance r_{12} was demonstrated in [10]. It was shown that the QFM amplitude contains the factor $\partial\Psi/\partial r_{12}$ at $r_{12} = 0$, which is connected to the function $\Psi(r_1,r_1,r_{12} = 0)$ by the Kato cusp condition [11]. The latter appears to be very important for calculation of the QFM amplitude [7]. We employ a very precise wave function [12] which also satisfies the Kato cusp conditions. We use an analytical function which approximates these wave functions at the electron coalescence line $r_{12} = 0$ very accurately [13].

We include only the quadrupole part of the electron-photon interaction. Note that the amplitude also contains the dipole terms proportional to the product $(\mathbf{e}\cdot\mathbf{q})$ with $\mathbf{e}$ the vector of the photon polarization. However, at least in the leading approximation, it is canceled by the contribution in which the electrons exchange by large momentum in the final state [7]. Anyway, in the experiments [1–3] the observations were carried out in the plane where $(\mathbf{e}\cdot\mathbf{q}) = 0$. Thus we can focus on the quadrupole contribution.

Besides the conservation of the linear momentum expressed by Eq. (2) we write the energy conservation condition

$$\omega - I = E, \quad E = \varepsilon_1 + \varepsilon_2, \tag{3}$$

where $\varepsilon_i = p_i^2/2m$ $(i = 1,2)$ are the photoelectron energies. Note that in our system of units $\omega = |\mathbf{k}|$.

To simplify the calculations we restrict ourselves to the case when the photon wavelength is much larger than the size of the bound state, i.e.,

$$\omega \ll \mu. \tag{4}$$

For the helium atom this means that $\omega \ll 6$ keV. Under this condition, Eq. (2) can be written as

$$\mathbf{q} = -\mathbf{p_1} - \mathbf{p_2}, \tag{5}$$

in the lowest order of expansion in powers of k.

Momentum q can become as small as μ only if momenta of the outgoing electrons almost compensate for each other, i.e., $|\mathbf{p_1} + \mathbf{p_2}| \sim \mu \ll p_{1,2}$. Hence, the photoelectrons are emitted mostly "back to back," with $t \equiv (\mathbf{p_1}\cdot\mathbf{p_2})/p_1p_2$ close to -1, while the values $p_1 \approx p_2$, i.e., $|p_1 - p_2| \ll p_{1,2}$. Thus the relative difference of the energies of the outgoing electrons

$$\beta \equiv \frac{|\varepsilon_1 - \varepsilon_2|}{E} \tag{6}$$

should be small. Since $q \geqslant |p_1 - p_2|$, we find

$$\beta < \frac{q}{(mE)^{1/2}} \ll 1. \tag{7}$$

This equation is presented in the lowest order in β.

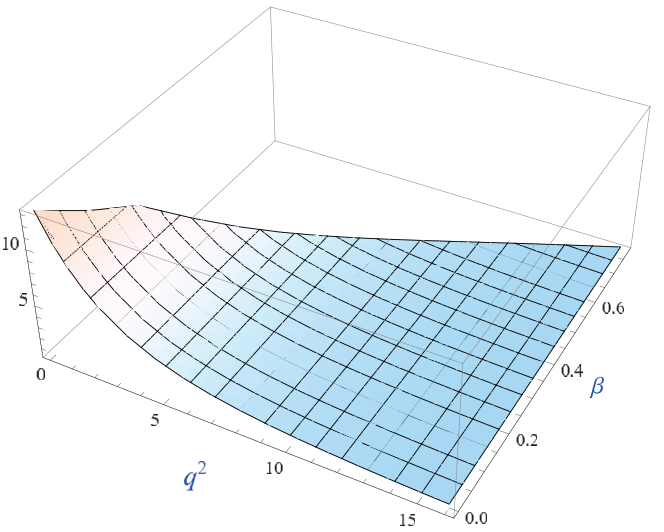

FIG. 1. (Color online) Distribution $d\sigma^{2+}/dq^2d\beta$ in $10^{-10}r_0^4$, $r_0 = 1/m\alpha$ for $\omega = 800$ eV. The recoil momentum q is in atomic units.

Besides the distributions $d\sigma^{2+}/dq^2d\varepsilon$ and $d\sigma^{2+}/dq^2$ (Figs. 1–3), we calculate the differential cross sections $d\sigma^{2+}/dtd\varepsilon$ and $d\sigma^{2+}/dt$ (Figs. 4–6). We present the numerical data for the photons carrying the energy of about 1 keV, employed in the experiments [1–3].

Note that this approach was used in [14] for calculation of the distributions $d\sigma^{2+}/dtd\varepsilon$ and $d\sigma^{2+}/d\varepsilon$ at the point of the peak $t = -1$. In other words, in [14] the height of the peaks of these distributions was found. In the present paper we calculate the shape of the peaks.

II. GENERAL EQUATIONS

The differential cross section of the double photoionization can be written as

$$d\sigma^{2+} = \frac{1}{2\omega}|F(\mathbf{k},\mathbf{p_1},\mathbf{p_2})|^2 d\Gamma. \tag{8}$$

Here $F(\mathbf{k},\mathbf{p_1},\mathbf{p_2})$ is the amplitude of the process. Averaging over polarizations of the photon is assumed. The last factor is

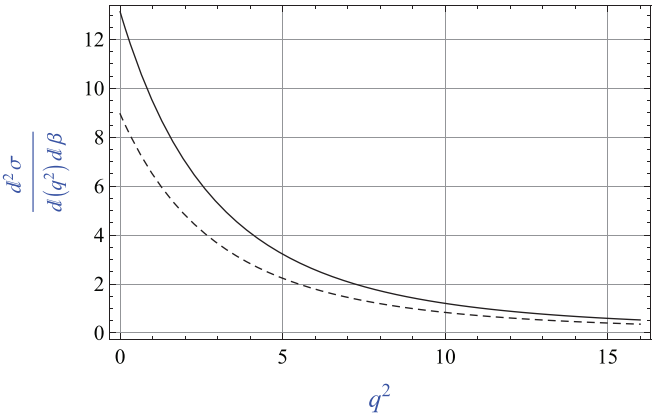

FIG. 2. (Color online) Distribution $d\sigma^{2+}/dq^2d\beta$ in $10^{-10}r_0^4$, $r_0 = 1/m\alpha$ for $\beta = 0$. Solid line is for $\omega = 800$ eV, dashed line is for $\omega = 1$ keV. The recoil momentum q is in atomic units.

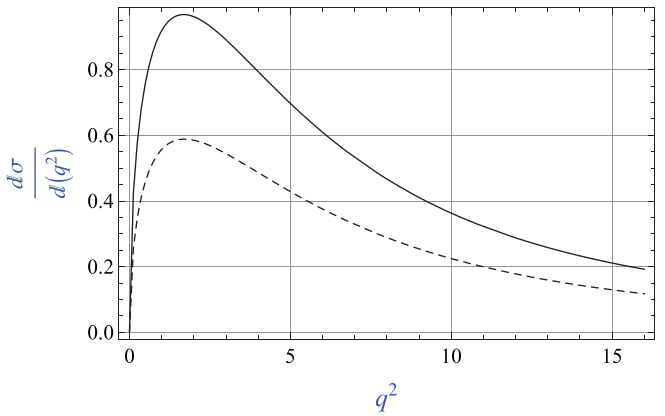

FIG. 3. (Color online) Distribution $d\sigma^{2+}/dq^2$ in $10^{-10}r_0^4$, $r_0 = 1/m\alpha$. Notations are the same as in Fig. 2.

the phase volume

$$d\Gamma = 2\pi\delta(\omega - I - \varepsilon_1 - \varepsilon_2)\frac{d^3p_1}{(2\pi)^3}\frac{d^3p_2}{(2\pi)^3}. \tag{9}$$

Employing Eq. (5), we can present

$$d\Gamma = \delta\left(\omega - I - 2\varepsilon_1 - \frac{p_1 q_z}{m} - \frac{q^2}{2m}\right)\frac{dq^2 dq_z}{4\pi}\frac{d^3p_1}{(2\pi)^3} \tag{10}$$

with z the direction of momentum $\mathbf{p_1}$. Using the δ function for integration over q_z we can write

$$d\sigma^{2+} = |F(\mathbf{k},\mathbf{p_1},\mathbf{p_2})|^2\frac{\theta(q/p-\beta)}{8\pi}\frac{Em^2}{\omega}\frac{d\beta}{2\pi}\frac{d\Omega}{4\pi}\frac{dq^2}{2\pi}, \tag{11}$$

with Ω the solid angle of the photoelectron with momentum $\mathbf{p_1}$, $p = (mE)^{1/2}$.

The amplitude of the process can be written as

$$F(\mathbf{k},\mathbf{p_1},\mathbf{p_2}) = \langle\Psi_f(1,2)|\gamma_1 + \gamma_2|\Psi_i(1,2)\rangle, \tag{12}$$

where the numbers 1 and 2 denote the variables corresponding to two electrons, $\Psi_{i,f}$ are the wave functions of the initial and final states, and

$$\gamma = (4\pi\alpha)^{1/2}e^{i(\mathbf{k}\cdot\mathbf{r})}\frac{-i(\mathbf{e}\cdot\nabla)}{m}, \tag{13}$$

where $\mathbf{e}$ is the vector of polarization of the photon, $(\mathbf{e}\cdot\mathbf{k}) = 0$. Recall that we shall pick only the quadrupole terms of interaction between the photon and electron. For further evaluation we denote

$$F(\mathbf{k},\mathbf{p_1},\mathbf{p_2}) = (4\pi\alpha)^{1/2}M(\mathbf{k},\mathbf{p_1},\mathbf{p_2}). \tag{14}$$

As we said earlier, we describe the final state by the function

$$\Psi_f(\mathbf{r_1},\mathbf{r_2}) = \frac{1}{\sqrt{2}}[(\psi_1(\mathbf{r_1})\psi_2(\mathbf{r_2}) + \psi_2(\mathbf{r_1})\psi_1(\mathbf{r_2})], \tag{15}$$

where ψ_i are the single-particle nonrelativistic Coulomb field functions with asymptotic momenta $\mathbf{p_i}$. We shall need the

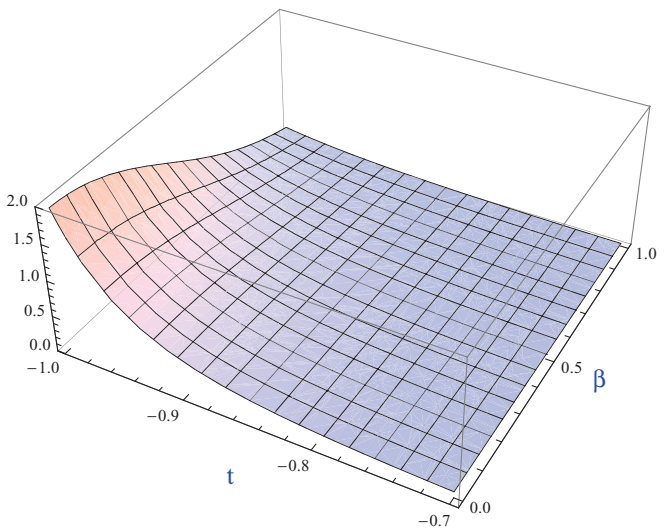

FIG. 4. (Color online) Distribution $d\sigma^{2+}/dtd\beta$ in barns for $\omega =$ 800 eV.

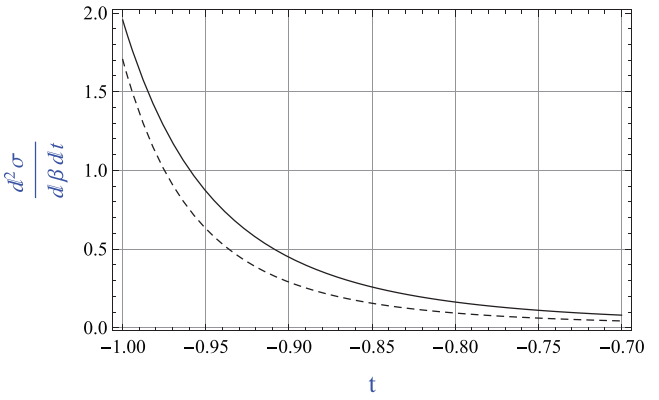

FIG. 5. (Color online) Distribution $d\sigma^{2+}/dtd\beta$ in barns for $\beta =$ 0. Notations are the same as in Fig. 2.

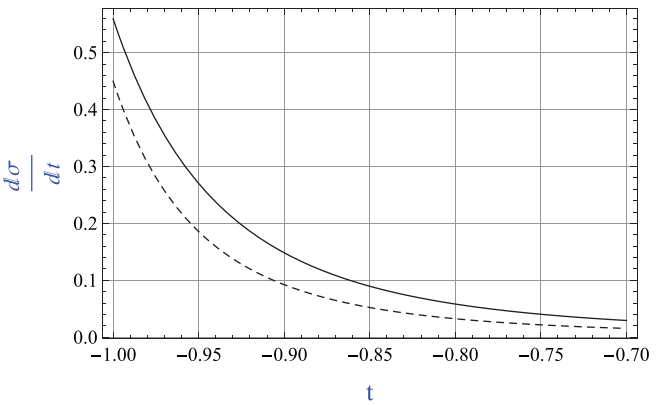

FIG. 6. (Color online) Distribution $d\sigma^{2+}/dt$ in barns for $\beta = 0$. Notations are the same as in Fig. 2.

functions

$$\psi^*_{\mathbf{p_i}}(\mathbf{r}) = e^{-i(\mathbf{p_i}\cdot\mathbf{r})}X(\mathbf{p_i},\xi_i,\mathbf{r}), \quad i = 1,2. \tag{16}$$

Here

$$X(\mathbf{p_i},\xi_i,\mathbf{r}) = N(\xi_i)_1F_1(i\xi_i,1,ip_ir + i(\mathbf{p_i}\cdot\mathbf{r})), \tag{17}$$

while

$$N(\xi_i) = \left(\frac{2\pi\xi_i}{1-e^{-2\pi\xi_i}}\right)^{1/2}, \tag{18}$$

with

$$\xi_i = \frac{\eta}{p_i}, \quad \eta = m\alpha Z. \tag{19}$$

Here Z is the charge of the nucleus. Note that in the hydrogenlike approximation, η is the averaged momentum of the electron in the $1s$ state.

Thus

$$\begin{aligned} M(\mathbf{k},\mathbf{p_1},\mathbf{p_2}) &= \sqrt{2}[A(\mathbf{k},\mathbf{p_1},\mathbf{p_2}) + (\mathbf{p_1} \longleftrightarrow \mathbf{p_2})], \\ A(\mathbf{k},\mathbf{p_1},\mathbf{p_2}) &= \int d^3r_1d^3r_2e^{i(\mathbf{k}\cdot\mathbf{r_1})-i(\mathbf{p_1}\cdot\mathbf{r_1})-i(\mathbf{p_2}\cdot\mathbf{r_2})}X_1(\mathbf{r_1})X_2(\mathbf{r_2}) \\ &\quad\times\left(\mathbf{e}\cdot\nabla_{\mathbf{r_1}}\right)\Psi_i(\mathbf{r_1},\mathbf{r_2}) \equiv A. \end{aligned} \tag{20}$$

Here we denoted

$$X_i(\mathbf{r}) = X(\mathbf{p_i},\xi_i,\mathbf{r}). \tag{21}$$

We introduce

$$\mathbf{R} = \frac{\mathbf{r}_1+\mathbf{r}_2}{2}, \quad \boldsymbol{\rho} = \mathbf{r}_2 - \mathbf{r}_1. \tag{22}$$

Presenting

$$\mathbf{r}_1 = \mathbf{R} - \boldsymbol{\rho}/2, \quad \mathbf{r_2} = \mathbf{R} + \boldsymbol{\rho}/2, \quad \nabla_{r_1} = \tfrac{1}{2}\nabla_R - \nabla_\rho, \tag{23}$$

and

$$\Psi_i(\mathbf{r_1},\mathbf{r_2}) = \Psi(\mathbf{R},\boldsymbol{\rho}), \tag{24}$$

we obtain

$$A = A_1 + A_2, \tag{25}$$

with

$$\begin{aligned} A_1 &= \frac{i}{m}\int d^3Rd^3\rho e^{-i(\mathbf{a}\cdot\boldsymbol{\rho})+i(\mathbf{q}\cdot\mathbf{R})} \\ &\quad\times X_1\left(\mathbf{R}-\frac{\boldsymbol{\rho}}{2}\right)X_2\left(\mathbf{R}+\frac{\boldsymbol{\rho}}{2}\right)(\mathbf{e}\cdot\nabla_\rho)\Psi(\mathbf{R},\boldsymbol{\rho}), \end{aligned} \tag{26}$$

while

$$\begin{aligned} A_2 &= -\frac{i}{2m}\int d^3Rd^3\rho e^{-i(\mathbf{a}\cdot\boldsymbol{\rho})+i(\mathbf{q}\cdot\mathbf{R})} \\ &\quad\times X_1\left(\mathbf{R}-\frac{\boldsymbol{\rho}}{2}\right)X_2\left(\mathbf{R}+\frac{\boldsymbol{\rho}}{2}\right)(\mathbf{e}\cdot\nabla_R)\Psi(\mathbf{R},\boldsymbol{\rho}), \end{aligned} \tag{27}$$

where

$$\mathbf{a} = \frac{\mathbf{p}_1-\mathbf{p}_2+\mathbf{k}}{2}, \quad a = |\mathbf{a}|. \tag{28}$$

Since $a \gg q$, the integrals on the right-hand sides of Eqs. (26) and (27) are saturated by $R \sim 1/q \gg \rho$. Thus we can set $\boldsymbol{\rho} = 0$ in the functions X_i. This provides

$$A_1 = \frac{(\mathbf{e}\cdot\mathbf{a})}{m}\int d^3Re^{i(\mathbf{q}\cdot\mathbf{R})}X_1(\mathbf{R})X_2(\mathbf{R})\int d^3\rho e^{-i(\mathbf{a}\cdot\boldsymbol{\rho})}\Psi(\mathbf{R},\boldsymbol{\rho}). \tag{29}$$

Now we expand the wave function

$$\begin{aligned} \Psi(\mathbf{R},\boldsymbol{\rho}) = \Psi(R,\tau,\rho) &= \Psi(R,0,0) + \tau\Psi'_\tau(R,\tau,0) \\ &\quad + \rho\Psi'_\rho(R,0,\rho) + 0(\rho^2). \end{aligned} \tag{30}$$

Here $\tau = (\mathbf{R}\cdot\boldsymbol{\rho})$, the derivatives are taken at $\tau = \rho = 0$.

We can calculate the integral over ρ multiplying the integrand by $e^{-\nu\rho}$ and putting $\nu = 0$ in the final step:

$$\begin{aligned} \int d^3\rho e^{-i(\mathbf{a}\cdot\boldsymbol{\rho})}\Psi(\mathbf{R},\boldsymbol{\rho}) &= \int d^3\rho e^{-i(\mathbf{a}\cdot\boldsymbol{\rho})-\nu\rho}\Psi(\mathbf{R},\boldsymbol{\rho}=0) \\ &= \int d^3\rho e^{-i(\mathbf{a}\cdot\boldsymbol{\rho})-\nu\rho}\rho\Psi'_\rho(R,0,\rho=0) \\ &= -\frac{8\pi\Psi'_\rho(R,0,\rho=0)}{a^4}. \end{aligned} \tag{31}$$

The derivative Ψ_ρ at $\rho = 0$ is related to the wave function by the Kato cusp condition [13]

$$\lim_{\rho\to 0} r_0\Psi'_\rho(\mathbf{R},\boldsymbol{\rho}) = \tfrac{1}{2}\Psi(R,0), \tag{32}$$

where $r_0 = 1/m\alpha$ is the Bohr radius. It is identical to similar relation for the wave function presented in variables r_1,r_2,ρ. Introducing

$$\Phi(R) = \Psi(\mathbf{R},\boldsymbol{\rho}=0), \tag{33}$$

we can write

$$A_1 = \frac{4\pi\alpha}{a^4}(\mathbf{e}\cdot\mathbf{a})S_1(q), \tag{34}$$

with

$$S_1(q) = \int d^3Re^{i(\mathbf{q}\cdot\mathbf{R})}X_1(\mathbf{R})X_2(\mathbf{R})\Phi(R), \tag{35}$$

with the functions $X_i(\mathbf{R})$ defined by Eq. (21).

Combining Eqs. (14), (20), (25), and (28), we find for the quadrupole terms of the amplitude

$$F(\mathbf{k},\mathbf{p_1},\mathbf{p_2}) = (4\pi\alpha)^{3/2}4\sqrt{2}\frac{(\mathbf{e}\cdot\mathbf{n})(\mathbf{k}\cdot\mathbf{n})}{p^4}S_1(q). \tag{36}$$

After averaging over the photon polarization and integration over the angles Eq. (11) takes the form

$$\frac{d^2\sigma}{dq^2d\beta} = \frac{2^7}{15}\alpha^3\frac{\omega}{E^4}|S_1(q)|^2. \tag{37}$$

In order to calculate $S_1(q)$ we employ the presentation of the function

$$\Phi(R) = c_1e^{-\lambda_1R} + c_2e^{-\lambda_2R}, \tag{38}$$

with numerical values of the parameters

$$c_1 = 0.380\zeta^3, \quad c_2 = 0.990\zeta^3, \quad \lambda_1 = 5.54\zeta,$$
$$\lambda_2 = 3.41\zeta, \quad \zeta = m\alpha$$

found in [13].

Further calculations are described in the Appendix. We obtain for the function $S_1(q)$ defined by Eq. (35)

$$|S_1(q)|^2 = \left| \sum_i c_i I(\lambda_i) \right|^2, \quad i = 1,2, \tag{39}$$

with $I(\lambda_i)$ defined by Eq. (A11).

III. RESULTS

Now we present the results of the computations. The cross section $d^2\sigma/dq^2 d\beta$ determined by Eq. (37) is presented in a three-dimensional Fig. 1 for $\omega = 800$ eV. As expected, it obtains the largest values at small $\beta \ll 1$ and in the region of small $q \sim 1$ a.u. in agreement with the experimental results [3]. This distribution at $\beta = 0$, corresponding to the center of the spectrum is shown in Fig. 2 for $\omega = 800$ eV and $\omega = 1$ keV. Since the effects of finite β manifest themselves in the terms of the order β^2, there is no noticeable difference from similar figures for $\beta \neq 0$ in the QFM region due to Eq. (7).

It is instructive also to view the energy distribution of the angular correlation

$$\frac{d^2\sigma}{dt d\beta} = 2p_1 p_2 \frac{d^2\sigma}{dq^2 d\beta}, \quad t = \frac{(\mathbf{p_1} \cdot \mathbf{p_2})}{p_1 p_2}. \tag{40}$$

It is shown for $\omega = 800$ eV in the three-dimensional Fig. 4. As expected, the largest values are reached at $\beta \ll 1$ and t close to -1, corresponding to the electrons ejected in the opposite directions (back to back). For $\beta = 0$ this differential cross section is shown in Fig. 5 for $\omega = 800$ eV and $\omega = 1$ keV.

We also calculate the distribution in recoil momentum

$$\frac{d\sigma}{dq^2} = \frac{1}{2} \int_0^{q/p} d\beta \frac{d^2\sigma}{dq^2 d\beta}, \tag{41}$$

and the angular correlation

$$\frac{d\sigma}{dt} = \frac{1}{2} \int_0^1 d\beta \frac{d^2\sigma}{dt d\beta}. \tag{42}$$

They are presented in Figs. 3 and 6, correspondingly. As expected, the distribution $d\sigma/dq^2$ has a local maximum at q about 1 a.u.. At $q = 0$ this distribution turns to zero just because the interval of integration over β vanishes. The angular correlation $d\sigma/dt$ has a sharp peak at $t = -1$, in agreement with the previous analysis.

IV. SUMMARY

We calculated the distributions in recoil momenta q and their energy distribution for the high-energy nonrelativistic double photoionization of helium caused by the QFM [4]. They are closely related to the distributions in the angle between momenta of the outgoing electrons (angular correlations). As expected, the distributions in recoil momenta obtain local maxima at small q of the order $1 - 2$ a.u., in agreement with the results of the pioneering experiments [1–3]. Unfortunately, the way the results in [1–3] are presented does not permit comparison of the quantitative results. The corresponding angular distributions obtain maxima when the photoelectrons move in the opposite directions (back-to-back scattering). The qualitative picture is the same for heavier atoms.

The QFM is caused by the initial state interactions and, contrary to a misleading statement in [3], is contained in the standard Feynman diagrams for the amplitude [4]. Since the QFM is at work at small separation between the bound electrons r_{12}, we described the initial state by a very precise wave function [12], employing its analytical approximation at small values of r_{12} [13]. We neglected the electron interactions in the final state. The numerical results for the photon energies in the keV region are shown in Figs. 1 through 6. This energy region attracts attention nowadays in connection with the laser experiments. Also, the experiments [1–3] were carried out at these energies. The approach can be applied for the double photoionization of heavier atoms.

The results show that it is not necessary to go to very large energies to find manifestation of the QFM. It manifests itself in the distributions in recoil momenta at the energies of the order of 1 keV.

One can obtain more precise results by directly employing precise wave functions, i.e., those found in [8]. However, such approaches do not allow analysis of the mechanisms of the process. On the other hand, very "accurate" wave functions (i.e., those which reproduce the value of the binding energy very accurately) may have a wrong behavior at $r_{12} \to 0$. It was demonstrated in [7,16] that a number of publications on the subject employing such functions contain erroneous results. More examples are given in [17]. That is why we consider our results to be a necessary step in the investigation of the process.

There are a number of possibilities to carry out the experimental investigation of other phenomena connected with the QFM. Outside the plane $(\mathbf{e} \cdot \mathbf{q}) = 0$ interference between the dipole and quadrupole terms should manifest itself in the angular distributions. Also, it would be interesting to trace the ω dependence of the shape of the energy distribution. Its theoretical analysis was presented in [17].

ACKNOWLEDGMENTS

The work was supported by the MSTI-RFBR Grant No. 11-02-92484. One of us (E.G.D.) gives thanks for hospitality during the visit to the Hebrew University of Jerusalem.

APPENDIX

Thus we calculate the integral

$$S_1(q) = \int d^3R e^{i(\mathbf{q}\cdot\mathbf{R})} X_1(\mathbf{R}) X_2(\mathbf{R}) e^{-\lambda R} = N(\xi_1) N(\xi_2) I(\lambda), \tag{A1}$$

where

$$I(\lambda) = \frac{-\partial J(\lambda)}{\partial \lambda}, \quad J(\lambda) = \int d^3R e^{i(\mathbf{q}\cdot\mathbf{R})} F_1(\mathbf{R}) F_2(\mathbf{R}) \frac{e^{-\lambda R}}{R}, \tag{A2}$$

with

$$F_i = {}_1F_1(i\xi_i,1,ip_iR + i(\mathbf{p_i}\cdot\mathbf{R})), \tag{A3}$$

The integral $J(\lambda)$ was calculated in [15] as

$$J(\lambda) = \frac{2\pi e^{-\pi\xi_1}}{\alpha_c}\left(\frac{\alpha_c}{\gamma_c}\right)^{i\xi_1}\left(\frac{\gamma_c+\delta_c}{\gamma_c}\right)^{-i\xi_2} {}_2F_1(1-i\xi_1,i\xi_2,1,g), \tag{A4}$$

with

$$\begin{aligned} &\alpha_c = \frac{q^2+\lambda^2}{2}, \quad \beta_c = (\mathbf{p_2}\cdot\mathbf{q}) - i\lambda p_2, \\ &\gamma_c = -(\mathbf{p_1}\cdot\mathbf{q}) + i\lambda p_1 - \alpha_c, \\ &\delta_c = p_1p_2 - (\mathbf{p_1}\cdot\mathbf{p_2}) - \beta_c, \quad g = \frac{\alpha_c\delta_c - \beta_c\gamma_c}{\alpha_c(\gamma_c+\delta_c)}. \end{aligned} \tag{A5}$$

We write Eq. (A4) in a more symmetric form,

$$J(\lambda) = \frac{2\pi e^{-\pi\xi_1}}{\alpha_c}\left(\frac{\alpha_c}{\gamma_c}\right)^{i\xi_1}\left(\frac{\alpha_c}{\alpha_c+\beta_c}\right)^{i\xi_2} {}_2F_1(i\xi_1,i\xi_2,1,h), \tag{A6}$$

with

$$h = \frac{\beta_c\gamma_c - \alpha_c\delta_c}{\gamma_c(\alpha_c+\beta_c)}. \tag{A7}$$

Thus

$$J(\lambda) = 4\pi\,\Lambda(\lambda)\,{}_2F_1(i\xi_1,i\xi_2,1,h(\lambda)), \tag{A8}$$

with

$$\begin{aligned} \Lambda(\lambda) = {} & (q^2+\lambda^2)^{-1+i\xi_1+i\xi_2}(p_1+p_2+i\lambda)^{-i\xi_1-i\xi_2} \\ & \times (p_2-p_1-i\lambda)^{-i\xi_1}(p_1-p_2-i\lambda)^{-i\xi_2}. \end{aligned} \tag{A9}$$

Employing

$$\frac{\partial}{\partial h}\,{}_2F_1(i\xi_1,i\xi_2,1,h) = -\xi_1\xi_2\,{}_2F_1(i\xi_1+1,i\xi_2+1,2,h), \tag{A10}$$

we find

$$I(\lambda) = \frac{8\pi\lambda}{(q^2+\lambda^2)^2}\Theta^{i(\xi_1+\xi_2)}(\lambda)T(\lambda)e^{-\pi/2(\xi_1+\xi_2)}. \tag{A11}$$

Here

$$\begin{aligned} &\Theta(\lambda) = \frac{q^2+\lambda^2}{s(\lambda)u(\lambda)}, \quad s(\lambda) = \sqrt{(p_1+p_2)^2+\lambda^2}, \\ &u(\lambda) = \sqrt{(p_1-p_2)^2+\lambda^2} \end{aligned} \tag{A12}$$

while

$$\begin{aligned} T(\lambda) = {} & \left(1 - \frac{i(\xi_1+\xi_2)}{2}\right)\{[1+h(\lambda)]\,{}_2F_1(i\xi_1,i\xi_2,1,h(\lambda)) \\ & - \xi_1\xi_2 h(\lambda)[1-h(\lambda)]\,{}_2F_1(i\xi_1+1,i\xi_2+1,2,h(\lambda))\}, \end{aligned} \tag{A13}$$

with

$$h(\lambda) = 1 - \frac{q^2+\lambda^2}{u^2(\lambda)}. \tag{A14}$$

[1] M. S. Schöffler *et al.*, ICPEAC 2011 (http://www.qub.ac.uk/icpeac2011/).
[2] Th. Weber *et al.*, Bull. Amer. Phys. Soc. **60**, 144 (2011).
[3] M. S. Schöffler *et al.*, arXiv:1207.7181 (2012).
[4] M. Ya. Amusia, E. G. Drukarev, V. G. Gorshkov, and M. P. Kazachkov, J. Phys. B **8**, 1248 (1975).
[5] Z. J. Teng and R. Shakeshaft, Phys. Rev. A **49**, 3597 (1994).
[6] E. G. Drukarev, Phys. Rev. A **52**, 3910 (1995).
[7] E. G. Drukarev, N. B. Avdonina, and R. H. Pratt, J. Phys. B **34**, 1 (2001).
[8] J. A. Ludlow, J. Colgan, T. G. Lee, M. S. Pindzola, and F. Robicheaux, J. Phys. B **42**, 225204 (2009).
[9] A. G. Galstyan, O. Chuluunbaatar, Yu. V. Popov, and B. Piraux, Phys. Rev. A **85**, 023418 (2012).
[10] T. Suric, E. G. Drukarev, and R. H. Pratt, Phys. Rev. A **67**, 022709 (2003).
[11] T. Kato, Commun. Pure Appl. Math. **10**, 151 (1957).
[12] E. Z. Liverts and N. Barnea, Comput. Phys. Commun. **182**, 1790 (2011).
[13] E. Z. Liverts, M. Ya. Amusia, R. Krivec, and V. B. Mandelzweig, Phys. Rev. A **73**, 012514 (2006).
[14] M. Ya. Amusia, E. G. Drukarev, and E. Z. Liverts, JETP Lett. **96**, 72 (2012).
[15] A. Nordsieck, Phys. Rev. **93**, 785 (1954).
[16] M. Ya. Amusia, E. G. Drukarev, and V. B. Mandelzweig, Phys. Scr. **72**, C22 (2005).
[17] E. G. Drukarev, Phys. Usp. **50**, 835 (2007).